PCCP

Accepted Manuscript

ROYAL SOCIETY OF CHEMISTRY

www.rsc.org/pccp

Cite this: DOI: 10.1039/c0xx00000x

www.rsc.org/xxxxxx

ARTICLE TYPE

Exploration of the binding interaction of a potential nervous system stimulant with calf-thymus DNA and dissociation of the drug-DNA complex by detergent sequestration

Pronab Kundu[a], Saptarshi Ghosh[a,*] and Nitin Chattopadhyay[a,*]

Received (in XXX, XXX) Xth XXXXXXXXX 20XX, Accepted Xth XXXXXXXXX 20XX
DOI: 10.1039/b000000x

Binding interaction of a potential nervous system stimulant, 3-acetyl-4-oxo-6,7-dihydro-12H indolo-[2,3-a] quinolizine (AODIQ), with calf-thymus DNA (ctDNA) has been explored thoroughly. The modified photophysics of the fluorescent molecule within the microheterogeneous biomacromolecular system has been exploited to divulge the drug-DNA binding interaction. The absorption and various fluorometric measurements together with the fluorescence quenching, urea-induced denaturation study, circular dichroism and DNA-melting studies unequivocally ascertain the mode of binding of the drug with the DNA to be groove binding. Corroborating the experimental observations, molecular docking simulation projects the minor groove of the biomacromolecule to be the site of binding. Further experiments have revealed that dissociation of the drug from the drug-DNA complex can be achieved by the detergent sequestration method. Besides providing an insight into the drug-DNA interaction the work also demonstrates the surfactant-induced excretion of the drug from the biomacromolecular assembly.

Introduction

Study of the interaction of small molecules with different biological targets is an emerging topic of interest to the biophysical researchers for the perception of structural and functional features of bio-macromolecules so as to simulate the biophysical processes.[1] Among the targets, deoxyribonucleic acid (DNA) is perhaps the most studied one since it controls the heredity of life by its base sequence and is also involved in many important biological processes like gene transcription,[2] mutagenesis,[3] gene expression,[4,5] etc. Spectroscopic elucidation of the interaction of small molecules with DNA not only provides insight into the drug-DNA binding phenomena, but also gives scope to develop new and effective therapeutic agents for countering various deadly diseases.[6] Small molecules bind to the DNA principally through two principal modes referred to as (i) intercalative binding where the molecule fits within the base pairs of the nucleic acid and (ii) groove binding involving non-bonding interactions with the deep major groove or the shallow minor groove of the DNA helix.[7,8] Several electronic and structural factors dictate the affinity, strength and mode of such binding interactions.[9,10] Unfortunately, so far no specificity has been resolutely enforced on the structure of the small molecules to predict with confidence its mode of binding with the DNA. However, it is well speculated fact that in general most of the planar aromatic molecules tend to bind with DNA by intercalative mode whereas crescent shaped molecules have a preference to bind through groove binding fashion.[11] For polar or cationic probes, a third type of binding mode *viz.* electrostatic binding with the negatively charged DNA phosphate backbone becomes obvious and it is also expected that such interaction can adequately alter the strength of intercalation or groove binding.[12,13]

In recent times, much attention has been focused on designing and synthesizing compounds having a wide range of pharmaceutical and pharmacokinetic properties and among them, indole derivatives are of great prospect. Compounds containing indole nucleus are potential agents for designing new derivatives that are able to protect the nervous system by interfering with the action of the reactive oxygen species (ROS) that participate in a number of pathological processes in the nervous system.[14] Molecules containing indole nucleus such as β-carbolines, indoleamines, carbazoles *etc.* are, by now, well-established bioactive molecules[14-18] and hence, it is relevant to explore the binding interaction of these potential drug molecules with appropriate biological targets. Interaction of carbazole with DNA has been studied by Wilson *et. al.*[19] where they have reported that the bioactive molecule binds to the minor groove of DNA. The potential central nervous system stimulant, β-carbolines encompass extensive pharmacological activities serving as, hallucinogens, paralysants of cardiac muscle, etc.[20,21] 3-acetyl-4-oxo-6,7-dihydro-12H indolo-[2,3-a] quinolizine (AODIQ, Scheme 1), possessing a similar basic skeleton to that of β-carboline is likely to have biological activity close to that of the latter in the same way as pyrimido pyridoindole has (see later, Scheme 2). AODIQ also shows a marked sensitivity towards the polarity of the medium[22] that enables this non-ionic molecular probe to study different microheterogeneous media to explore the

potential efficacy of its fluorescence properties for unearthing its interaction with relevant biological targets.[17,23-26] In the present contribution we have made a successful endeavor to demonstrate the binding interaction of AODIQ with the most relevant biological target, DNA, exploiting vivid spectroscopic as well as computational techniques. The modulated steady state and time resolved fluorometric responses of the probe in the ctDNA environment, determined binding constant, fluorescence quenching experiment, urea-induced denaturation study, circular dichroism (CD) spectral study and thermometric experiment relating to the helix melting of DNA unambiguously establish that AODIQ binds with ctDNA through groove binding mode. Molecular docking simulation corroborates the experimental results and provides a support to the proposition of groove binding of the drug in a nice way by projecting the minor groove region to be the most probable binding site of the drug in ctDNA. Effect of ionic strength of the medium on the probe-DNA assembly suggests that the change in the ionic strength of the solution has insignificant effect on the drug-DNA binding interaction. Further, aiming at our objective to reduce the drug-induced side effects through the excretion of the excess drugs from the body,[27-30] we have made an endeavor to dissociate the drug from the drug-DNA complex by the detergent sequestration method.[11] The present contribution is expected to provide an insight into the mode of binding of the β-carboline drugs with DNA or similar biological targets.

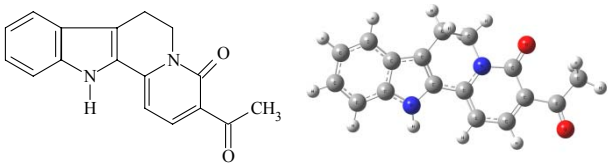

Scheme 1. Schematic and optimized structures of AODIQ.

Experimental

Materials

3-Acetyl-4-oxo-6,7-dihydro-12H indolo-[2,3-a] quinolizine (AODIQ) (Scheme 1) was synthesized using the method mentioned elsewhere.[31] It was purified by column chromatography, and the purity of the compound was checked by thin layer chromatography (TLC). ctDNA (Molecular wt. 8.4 MDa), Tris-HCl buffer and AR grade potassium iodide (KI) were obtained from Sisco Research Laboratories (SRL, India) and used as received. Cetyltrimethyl ammonium bromide (CTAB) and sodium chloride (NaCl) were procured from Sigma-Aldrich (USA). Urea (Merck, India) and spectroscopic grade 1,4-dioxane (Spectrochem, India) were used without further purification. Deionised water from a Milli-Q water purification system (Millipore) was used throughout the experiment. All the experiments were performed using Tris-HCl buffer of 0.01 M at pH = 7.1.

Stock solution of ctDNA was prepared by dissolving solid ctDNA in Tris-HCl buffer (pH = 7.1) and stored at 4 °C. The purity of ctDNA was verified by monitoring the ratio of absorbance at 260 nm to that at 280 nm, which was in the range 1.8—1.9. The concentration of ctDNA solution was determined spectrophotometrically using ε_{DNA} = 13,600 mol^{-1} dm^3 cm^{-1} at 258 nm.[32] The concentration of AODIQ was kept at 5 μM throughout the study unless otherwise specified. Freshly prepared solutions were used for all the measurements.

Methods

Shimadzu UV-2450 absorption spectrophotometer (Shimadzu Corporation, Kyoto, Japan) was used for the steady state absorption studies. Steady state fluorescence and fluorescence anisotropy measurements were carried out in a Horiba Jobin Yvon Fluoromax-4 spectrofluorometer. Fluorescence anisotropy (r) is defined as

$$r = (I_{VV} - G.\ I_{VH}) / (I_{VV} + 2G.\ I_{VH}) \qquad (1)$$

where I_{VV} and I_{VH} are the emission intensities obtained with the excitation polarizer oriented vertically and emission polarizer oriented vertically and horizontally, respectively. The G factor is defined as[33]

$$G = I_{HV}/ I_{HH} \qquad (2)$$

where the intensities I_{HV} and I_{HH} refer to the vertical and horizontal positions of the emission polarizer, with the excitation polarizer being horizontal.

Time resolved fluorescence decay measurements were performed by the time-correlated single photon counting (TCSPC) technique in Horiba Jobin Yvon FluoroCube fluorescence lifetime system using NanoLED at 370 nm (IBH, UK) as the excitation source and TBX photon detection module as the detector. The decays were analyzed using IBH DAS-6 decay analysis software. The lamp profile was collected by placing a scatterer (dilute micellar solution of sodium dodecyl sulfate in water) in place of the sample. Goodness of fits was evaluated from χ^2 criterion and visual inspection of the residuals of the fitted function to the data. Mean (average) fluorescence lifetimes (τ_{avg}) for biexponential iterative fittings were calculated from the decay times (τ_1 and τ_2) and the normalized pre-exponential factors (a_1 and a_2) using the following relation

$$\tau_{avg} = a_1\tau_1 + a_2\tau_2 \qquad (3)$$

Circular dichroism spectra were recorded on a JASCO J-815 spectropolarimeter (Jasco International Co., Hachioji, Japan) using a rectangular quartz cuvette of path length 1 cm. The CD profiles were obtained employing a scan speed of 50 nm/min and appropriate baseline corrections were made by using aqueous buffer solution. All the experiments were performed at room temperature (298 K) with air-equilibrated solutions.

For the DNA helix melting experiment, pre-fixed temperatures were set using a high precession peltier (Wavelength Electronics, USA, Model No. LFI-3751, temperature stability within 0.002^0C) that was attached to the aforesaid spectrophotometer.

For molecular docking simulation the crystal structure of DNA was taken from protein data bank (PDB) having PDB ID 1BNA (a dodecamer d(CGCGAATTCGCG)).[34] AutoDock-vina program (version 1.1.2) from The Scripps Research Institute[35] was used for the molecular docking calculations. As reported in the recent literatures, AutoDock vina provides better accuracy in predicting the binding mode than Autodock 4 sowtware.[35-37] For docking

study, the geometries of AODIQ and other molecular systems were first optimized using density functional theory (DFT) at the B3LYP/6-31G** level using Gaussian 03W program[38] and the output file was converted into a compatible PDB file. Before docking study, MGLTools (version 1.5.6) were used to convert the receptor and drug coordinate files into PDBQT format. A three dimensional grid box of 22×24×42 was created with a grid spacing of 1Å and centered on coordinates x = 14.682, y = 21.003 and z = 8.834. For allowing the drug molecule to travel around all the possible binding sites of DNA, this grid box included the entire DNA fragments. For docking simulation 20 different conformations were used to find out the lowest binding energy conformer. PyMOL software package was used for visualization and analyzing the docked conformations.[39]

Results and discussion

Steady state absorption and emission studies

The UV-vis absorption spectrum of AODIQ in aqueous buffer solution shows a broad and unstructured low energy band with λ_{abs}^{max} at ~ 420 nm as depicted in Figure 1.[23] Gradual addition of ctDNA to the buffered solution of AODIQ results in an appreciable decrease in the absorbance (Figure 1) and the concomitant development of two bands one on either side of the band maximum resulting in the observation of two isosbestic points. The set of observations indicates a binding interaction between AODIQ and the DNA. In spite of an appreciable modification of the absorption spectrum of the probe with the addition of DNA there is only a little red shift of the absorption maximum which primarily suggests groove binding of the drug with ctDNA, since it is an established fact that insignificant (or small) shift in absorption spectral behavior (i.e., λ_{abs}^{max}) is the most probable consequence of groove binding since intercalation of small molecules into the DNA base stack usually causes larger shift of the absorption maxima.[9,40-42] Existence of the isosbestic points implies that there is an equilibrium between the free and the DNA-bound probe in the ground state.

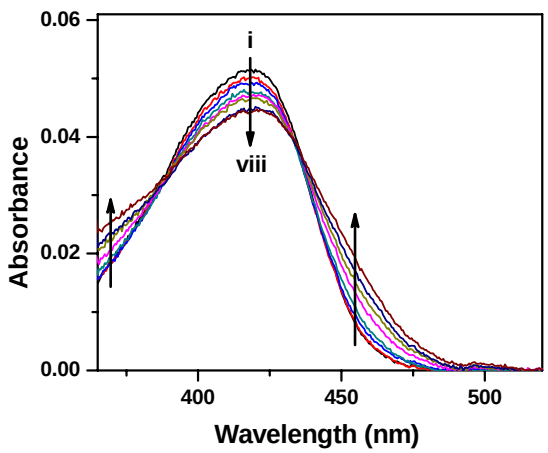

Figure 1. Absorption spectra of AODIQ in the aqueous buffer and in the presence of increasing concentrations of ctDNA. Curves i → viii correspond to [ctDNA] = 0, 0.083, 0.204, 0.283, 0.399, 0.511, 0.620, 0.690 mM. [AODIQ] = 5 µM.

The emission profile of the probe is found to reveal the consequences of the drug-DNA interaction more precisely. In aqueous buffer, the room temperature emission spectrum of AODIQ shows a single broad and unstructured band assigned to the charge transfer (CT) emission with a maximum at around 515 nm.[17,25] With increasing concentration of DNA, a prominent increase in the emission intensity along with an appreciable hypsochromic shift of the emission maximum (from 515 nm in aqueous buffer medium to 505 nm in 0.83 mM DNA) is observed. An isoemissive point is also developed at 556 nm implying the equilibrium between the unbound and the DNA-bound drug. Similar isoemissive points have also been observed for the same probe in micellar and protein media.[24,43] There is, however, no appreciable change in the width of the emission band as is evident from the calculation of the full width at half maximum (FWHM) of the emission bands of the probe in aqueous buffer and in different ctDNA solutions. Figure 2 presents the variation in the fluorescence spectra of AODIQ in the presence of added ctDNA. The fluorometric response of AODIQ in the DNA environment (both enhancement in the intensity and the blue shift of the emission maximum) indicates binding of the drug with the DNA. The considerable blue shift in the emission maximum of the drug in DNA medium suggests that the polarity of the environment around the drug is more hydrophobic (less polar) compared to that of the aqueous buffer milieu. The emission behavior of the drug in the DNA environment is in agreement with the characteristics of the drug in less polar media.[23,24-26]

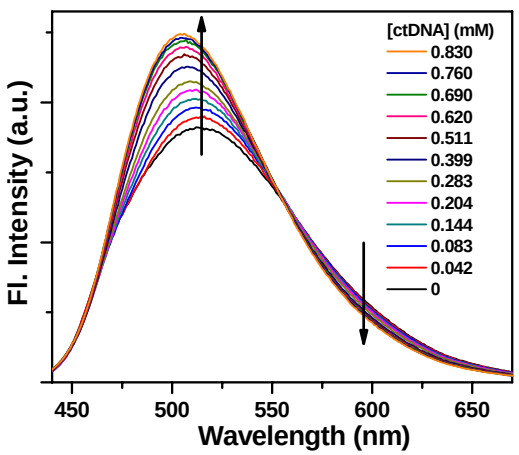

Figure 2. Emission spectra of AODIQ in presence of different concentrations of ctDNA. The concentrations of the ctDNA solutions are labeled in the legends. λ_{exc} = 420 nm, [AODIQ] = 5 µM.

In the present context, we have further estimated the polarity of the immediate environment around the drug in DNA medium by exploiting the sensitivity of its emission towards the medium polarity. Determination of the polarity in the immediate vicinity around the fluorophore is a convenient way to assess the location of the fluorophore within the microheterogeneous environment.[17,23] The micropolarities in such assemblies are often determined in terms of the standard $E_T(30)$ scale as developed by Kosower and Reichardt[44,45] by comparing the emission behavior of the fluorophore in the concerned microheterogeneous environment to that in a series of homogeneous solvent mixtures of varying composition with known $E_T(30)$ values. For the present purpose, a calibration plot monitoring the energies

corresponding to the fluorescence maxima of AODIQ in the water-dioxane mixtures of known $E_T(30)$ values has been constructed (Figure 3). Water/dioxane mixture was chosen for such studies over commonly used water/alcohol system since the former covers a much wider range of polarity.[32] Interpolation of the values of energies corresponding to the emission maxima of the drug in aqueous buffer and ctDNA environments on the calibration line gives the $E_T(30)$ values to be 60.9 (± 0.2) kcal mol^{-1} and 56.8 (± 0.2) kcal mol^{-1} respectively. It is important to note that due to possibilities of specific solvation of the probe in this solvent mixture as well as the gross approximation that the mixed solvents mimic the real bioenvironment, the obtained $E_T(30)$ values should be considered as qualitative ones. The study gives an indication that in DNA, the drug resides in a considerably less polar environment compared to the bulk aqueous medium. Thus, the micropolarity determination of the drug justifies its emission spectral shift of the drug (*vide infra*) in the DNA environment.

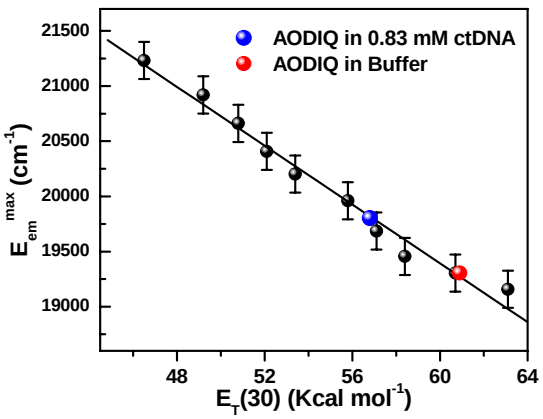

Figure 3. Variation of the energy corresponding to the maximum of the emission of AODIQ as a function of $E_T(30)$ in water-dioxane mixtures. The environments for the interpolated values are provided in the legends.

As the binding constant value provides an idea about the strength of binding between the probe and the macromolecule, and thereby gives a hint about the mode of binding, we have exploited the fluorescence titration data and the modified Benesi-Hildebrand equation[46] as given below, to determine the binding constant of the drug with the ctDNA.

$$\frac{1}{\Delta F} = \frac{1}{\Delta F_{max}} + \frac{1}{K\Delta F_{max}}\frac{1}{[L]} \qquad (4)$$

where $\Delta F = F_x - F_0$ and $\Delta F_{max} = F_\infty - F_0$ where F_0, F_x and F_∞ are the fluorescence intensities of AODIQ in the absence of ctDNA, at an intermediate ctDNA concentration and at a concentration for complete interaction respectively; K is the binding constant and [L] is the ctDNA concentration. The double reciprocal plot of $1/\Delta F$ against $[ctDNA]^{-1}$ gives a straight line (*vide* Figure 4) justifying a 1:1 interaction between the drug and the ctDNA. The excitation wavelength was set at 420 nm, the absorption maximum of the free AODIQ. Since there was a gradual decrease in the absorbance value with the addition of DNA, necessary corrections were incorporated in the emission intensities to accommodate the change in the absorbance at the excitation wavelength before using the values for calculation of the binding constant through the double reciprocal plot. The binding constant (K) is determined from the ratio of the intercept to the slope of the linear plot in Figure 4 and the value comes out to be 1.2×10^3 M^{-1} at 298 K. The order of the determined binding constant indicates groove binding of the drug with the DNA since for intercalative mode, the binding constants are known to be of much higher order (~ 10^5 M^{-1}).[47,48] From the estimated binding constant (K) value, free energy change for this AODIQ-DNA binding is calculated to be $\Delta G = -17.6$ kJ mol^{-1} dictating the process to be spontaneous.

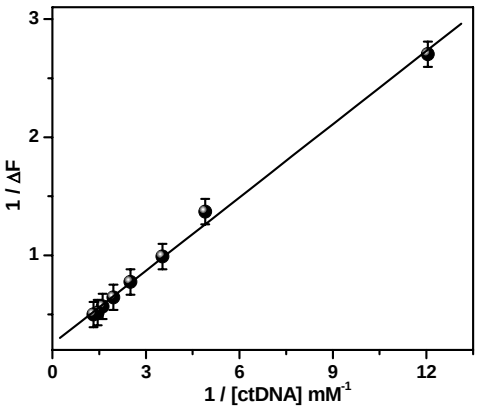

Figure 4. Double reciprocal plot for the binding of AODIQ with ctDNA.

Steady state fluorescence anisotropy study

Steady-state fluorescence anisotropy measurement reflects how the microheterogeneous environments impose motional restriction on the fluorophore and, thus, it is often probed to assess the motional information of the fluorophore in microheterogeneous environments like micelles, reverse micelles, lipids, proteins, cyclodextrins, DNA etc.[32,49] Fluorescence anisotropy of a fluorophore in fluid media where the fluorophore can rotate almost freely is very low while an increase in the rigidity in the microenvironment around the fluorophore causes an enhancement in the anisotropy value.[24-26,32] Figure 5 depicts the variation of the steady state fluorescence anisotropy of AODIQ with increasing ctDNA concentration. The figure reveals that with the gradual addition of DNA, the fluorescence anisotropy (r) of AODIQ increases monotonically before attaining a saturation demonstrating the imposition of motional restriction on the drug within the DNA environment. In ctDNA medium, similar value of anisotropy (r = 0.20) has been reported by Sahoo *et. al.* for 2-(4-(dimethylamino)styryl)-1-methylpyridinium iodide, a bioactive fluorophore used for the measurement of the membrane potential of living cells, that binds with DNA through groove binding mode.[9] It is also pertinent to mention here that AODIQ shows sufficiently high fluorescence anisotropy values in protein media[23] (0.34 in HSA and 0.32 in BSA) compared to the present case (r = 0.21). Had the binding of AODIQ with ctDNA been intercalative in nature, we would expect a even higher fluorescence anisotropy value since, for intercalated fluorophores, much higher fluorescence anisotropy values (~ 0.30) are generally observed.[49] Thus, the fluorescence anisotropy study suggests that the drug binds with the DNA

through groove binding fashion.

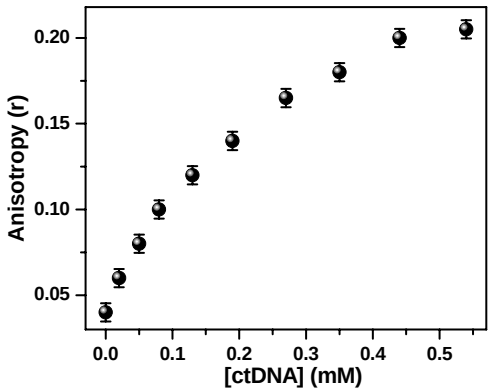

Figure 5. Variation of the steady state fluorescence anisotropy (r) of the drug as a function of DNA concentrations. λ_{exc} = 420 nm, λ_{em} = 515 nm. Each data point is an average of 10 individual measurements.

Fluorescence quenching study

To elucidate the mode of binding of the drug with ctDNA, we have also performed the fluorescence quenching study in both DNA environment and aqueous buffer medium using potassium iodide (KI) as a quencher. Considering the two different probable locations of the bound drug, i.e., intercalated into the DNA double strands or groove bound, the protection of the drug from the quencher is expected to be more in the former than the later situation.[11,32,49] Fluorescence quenching of AODIQ in aqueous buffer and DNA medium has been studied following the Stern-Volmer equation,

$$F_0/F = 1 + K_{SV}[Q] \quad (5)$$

$$\text{or, } F_0/F - 1 = K_{SV}[Q] \quad (6)$$

where F_0 and F are the fluorescence intensities in the absence and in the presence of the quencher KI (Q), [Q] is the molar concentration of the quencher and K_{SV} is the Stern-Volmer quenching constant. K_{SV} acts as an indicator to judge the exposure of the fluorophore to the quencher. Higher the value of K_{SV} higher is the degree of accessibility of the quencher to the fluorophore. Literature suggests that the K_{SV} values for the intercalated probe into the DNA account for the 5 − 8 times less compared to that in aqueous buffer medium.[42,49] Figure 6 represents the Stern-Volmer plots and depicts the relative extent of quenching of AODIQ in the aqueous buffer phase and in the DNA environment ([DNA] = 0.83 mM, this concentration is the saturation concentration of interaction between the drug and the DNA). The slopes of ($F_0/F - 1$) vs [KI] plots (Figure 6) yield the values of K_{SV} to be 10.12 M^{-1} and 5.73 M^{-1} for aqueous buffer and DNA medium respectively. The comparatively less lowering (a factor of 2 only) of the K_{SV} value of the drug in DNA medium relative to the aqueous buffer phase suggests that the mode of binding is groove binding in nature and not intercalative. From the fluorescence lifetime (τ) values of AODIQ in aqueous buffer and DNA environments (see Table 1) the quenching constants (k_q) have been estimated to be 1.1×10^{10} $M^{-1}s^{-1}$ and 3.8×10^9 $M^{-1}s^{-1}$ respectively in the respective media using the equation $k_q = K_{SV}/\tau$. The k_q values in both the media imply that the quenching processes are diffusion controlled.[33]

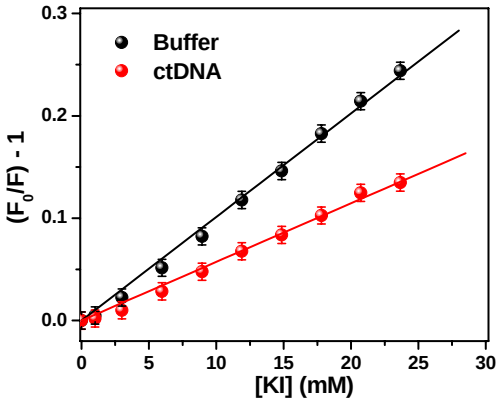

Figure 6. Stern-Volmer plots for the fluorescence quenching of AODIQ by I^- ion in aqueous buffer and DNA media as mentioned in the figure legends.

Time resolved fluorescence decay study

Fluorescence lifetime measurement serves as a tool to explore the local environment of the fluorophores within the microheterogeneous environments and it is sensitive to the excited state interactions.[23,26] To obtain a generalized picture of the drug-DNA interaction, we have recorded the fluorescence decays of AODIQ in the presence of varying concentrations of ctDNA. Characteristic decay profiles of AODIQ in the DNA environments are shown in Figure 7, and the deconvoluted data are compiled in Table 1. AODIQ shows biexponential decays both in aqueous medium as well as in the DNA environments. In aqueous buffer solution, existence of different hydrogen bonded species formed with the surrounded water molecules may be ascribed to be responsible for the biexponential decay behavior.[23] The bi- or multi- exponential decay of the polarity-sensitive fluorophore in microheterogeneous environments may originate from the location of the fluorophore in different polarity regions and is often observed for fluorophores in bio or biomimicking assemblies.[25,26,40,49] It is often difficult to provide specific mechanistic models to explain the individual components of the decays of a probe in complex microheterogeneous environments; it could even be misleading in some cases.[9,33,49] In the present case also we could not extract any realistic meaning from the analyses of the fluorescence decays. Hence, instead of putting emphasis on the individual decay constants we have used the average fluorescence lifetime of the probe to understand its gross behavior within the ctDNA environments relative to the buffer milieu.[9,33,49]

The average fluorescence lifetime of AODIQ increases regularly with increasing DNA concentration (Table 1). Similar observation for the same probe has already been reported in different microheterogeneous media like micelles, proteins, liposomes, cyclodextrins *etc*.[23,24-26]. Enhancement of the fluorescence lifetimes of other fluorophores in similar environments are also available in the literature.[11,50,51] A lowering in the polarity of the immediate vicinity around the probe is ascribed responsible for the observation. The time resolved measurements are, thus, consistent with the steady state fluorescence and micropolarity determination experiments.

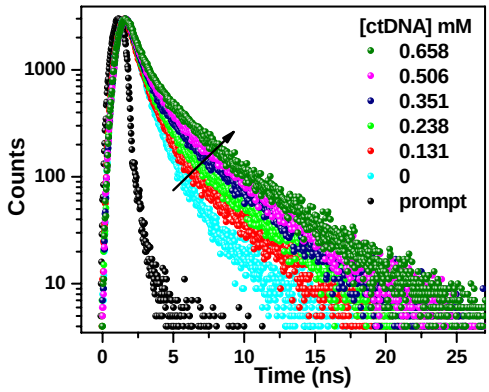

Figure 7. Time resolved fluorescence decay of AODIQ in presence of increasing DNA concentrations. The sharp profile (black) on the left is the lamp profile. The concentrations of the DNA solutions are labeled in the legends. λ_{exc} = 370 nm, λ_{em} = 515 nm.

Table 1. Time resolved fluorescence decay parameters of AODIQ in aqueous buffer and different DNA concentrations

Medium	τ_1 (ns)	a_1	τ_2 (ns)	a_2	τ_{avg} (ns)	χ^2
buffer	0.84	0.95	2.59	0.05	0.93	1.05
[ctDNA] (mM)						
0.05	0.87	0.96	3.55	0.04	0.98	1.05
0.13	0.87	0.92	3.70	0.08	1.09	1.12
0.24	0.86	0.90	3.87	0.10	1.16	1.00
0.35	0.89	0.87	4.03	0.13	1.30	1.15
0.50	0.90	0.84	4.11	0.16	1.41	1.06
0.66	0.91	0.81	4.14	0.19	1.52	1.19

Circular dichroism and helix melting studies

To confirm the mode of binding of the drug with the DNA, we have performed the circular dichroism (CD) and the DNA helix melting experiments. The secondary structure of DNA is known to be perturbed significantly by the intercalation with small molecules putting its signature through the changes in the intrinsic CD spectrum of DNA.[11,42,49] On the contrary, groove binding of the probes has insignificant effect on the CD profile of DNA.[9,40,52] The CD spectra of ctDNA in aqueous buffer medium in the absence and presence of varying drug concentrations are depicted in Figure 8 (A). The intrinsic CD spectrum of DNA consists of two peaks, one positive peak at around 275 nm and a negative peak around 245 nm, characteristic of the right handed B form.[42,52,53] Figure 8 (A) clearly demonstrates that successive addition of AODIQ to the DNA solution does not bring any significant change in the CD spectrum of DNA indicating that on binding with the drug, the secondary structure of the DNA remains practically unaffected. This observation categorically rules out the possibility of intercalation of AODIQ in the DNA helix, and thereby establishes that the drug binds to the DNA through groove binding mode.

The binding mode of the drug with DNA has further been substantiated from the DNA helix melting experiment. DNA melting is the process by which the hydrogen bonding and base stacking interactions between the strands of the double helix are disrupted by heating, resulting in the separation of the double helix into two single strands.[54] The melting temperature (T_m) of DNA is defined as the temperature at which half of this transition takes place.[52] Intercalation of probes into the DNA double helix increases the thermal stability of the helix by stabilizing the stacking interaction that causes an appreciable enhancement of the DNA melting temperature,[11,47,49] whereas, groove binding leads to an imperceptible modulation in the value of T_m.[32,40,52] In the present study, the melting profiles (Figure 8 (B)) for ctDNA in the absence and presence of the drug have been constructed by monitoring the DNA absorbance at 260 nm, which increases sharply as the helix melts.[52] We have determined T_m of both the native DNA and the drug bound DNA separately. The determined melting temperatures come out to be 71.0 (±0.2) ^{0}C and 71.3 (±0.2) ^{0}C in the absence and presence of the drug respectively. The result reveals that upon binding with AODIQ, T_m of DNA does not change significantly and hence, establishes the groove binding of the drug with the DNA.

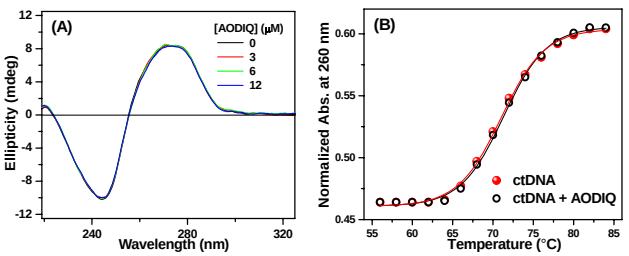

Figure 8. (A) Representative CD spectra of ctDNA with varying concentration of AODIQ. Concentrations of AODIQ are shown in the legends. [ctDNA] = 50 μM. (B) Thermal melting profiles of native ctDNA (20 μM) (red) and the same treated with 10 μM AODIQ (black).

Urea-induced denaturation study

It is well-known that destabilization of the double stranded DNA by denaturant leads to weakening of the drug-DNA binding resulting in the release of the entrapped drug molecules from the DNA environment to the bulk aqueous medium.[11,42] In the present project, urea induced denaturation study of the drug bound DNA have been exploited to confirm the drug-DNA binding. With the gradual addition of urea to the AODIQ-DNA complex, the fluorometric responses of AODIQ exhibit an opposite pattern to that observed while AODIQ binds to the DNA. With increasing concentration of urea, the emission intensity deceases steadily with a concomitant red shift of the emission maximum (from 505 nm in DNA environment to 514 nm in presence of 6 M urea) (Figure 9). These observations (both reduction in the fluorescence intensity and the red shift of the fluorescence maximum) clearly indicate that with the addition of urea DNA gets denatured leading to the release of the drug molecules from the DNA environment to the more polar bulk aqueous phase. It is important to note that at a considerably high denaturant concentration (6 M urea) the emission maximum of the drug (514 nm) matches closely to the value observed in the aqueous buffer milieu (515 nm). This can be rationalized by considering the fact that urea is able to denature the DNA to dislodge the drug almost completely from the DNA environment to the aqueous buffer medium.

Release of the drug to the bulk aqueous medium with the introduction of the denaturant (urea) is further corroborated by measuring the steady state fluorescence anisotropy of the drug with increasing urea concentration. With gradual addition of urea

to the drug-DNA complex, the fluorescence anisotropy of the drug progressively decreases, ultimately reaching a value of 0.06 at 8 M urea concentration (inset of Figure 9). This observation also confirms the release of the drug from the motionally constrained DNA environment to the bulk aqueous medium. However, a slight higher value of the fluorescence anisotropy of the drug in the presence of 8 M urea (r = 0.06) compared to that of the aqueous buffer (r = 0.04) may be attributed to the enhanced bulk viscosity of the medium due to the presence of 8 M urea.

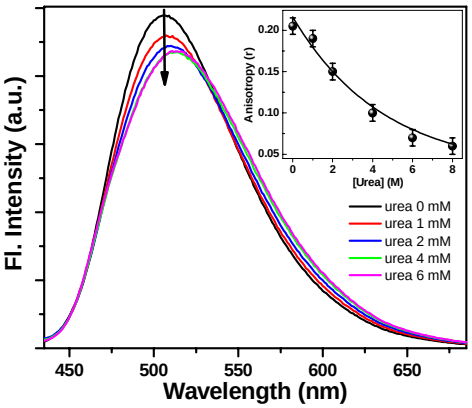

Figure 9. Variation of fluorescence intensity of DNA bound AODIQ as a function of urea concentration. Inset shows the variation of steady state fluorescence anisotropy of DNA bound AODIQ as a function of urea concentration. λ_{exc} = 420 nm, λ_{em} = 510 nm. Each data point is an average of 10 individual measurements.

Effect of ionic strength on drug-DNA binding

To verify whether there is significant electrostatic interaction between the drug and the DNA in the present case, we have studied the effect of ionic strength of the medium on the drug-DNA binding. Increased ionic strength of the medium screens the electrostatic repulsion between the neighboring phosphate groups, forcing the helix to shrink due to a reduction in the unwinding tendency caused by the electrostatic repulsion between the negatively charged intramolecular phosphate groups.[42] Hence, increased ionic strength of the solution leads to a weakening of the binding interaction between the positively charged molecules and DNA due to the reduced electrostatic attraction between them.[42,49] Upon gradual addition of sufficient concentration of NaCl (0.5 M) to the medium, the emission intensity of the DNA bound drug decreases only marginally without any noticeable shift of the emission maximum (Figure not shown). This observation indicates that there is no significant electrostatic contribution on the drug-DNA binding, which is consistent with the observation of single type of binding from the absorption study (*vide infra*). Similar non-dependence of probe-DNA binding on ionic strength of the medium has been reported by Mati *et. al.* for a neutral fluorophore.[40]

Molecular docking analysis

Since simulation can project the most probable site of the biomacromolecs towards the binding of a drug or probe, molecular docking has been established to serve as an efficient tool for the purpose in the advanced biophysical research.[9,40,52,55] To have a theoretical support in relation to the mode of binding of the drug with the DNA through finding the pragmatic binding location, we have performed the docking simulation study according to the protocol described in the Experimental section. It is important to keep in mind that the results of the docking analysis depends significantly on the chosen crystallographic structure of the DNA.[56] For our purpose, we have chosen B-DNA which is used by different research groups for finding the location of the bound probe in ctDNA.[9,40,52] The docked conformation (Figure 10) illustrates that AODIQ fits well in the natural curvature of the minor groove of the DNA. The computed docking energy for the docked conformation comes out to be – 30.5 kJ mol^{-1} which is in good agreement with the values of docking energies for the molecules that bind in a groove binding mode with ctDNA.[9,40] Thus, the molecular docking simulation corroborates the proposition of groove binding of the drug with DNA.

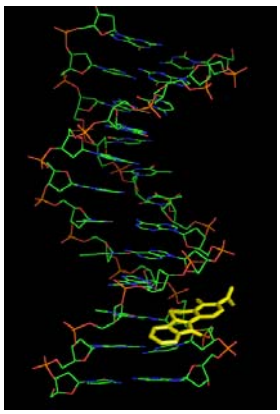

Figure 10. Optimized docked pose of AODIQ bound to the minor groove of B-DNA.

To compare the binding behavior of AODIQ with other central nervous system stimulants in DNA environments we have performed independent docking simulations with three different known nervous system stimulants, namely, indoleamine, carbazole and pyrimido pyridoindole.[14] It is known that the activity of a drug depends largely on its binding site in DNA.[57] So, it would be useful to compare the binding location of AODIQ with some known nervous system stimulants to check whether AODIQ binds with DNA in a similar position to that of the said compounds or not.

Among the three aforesaid molecular systems considered for comparison, carbazole is known to bind in the minor groove of DNA with free energy change of ~ 34 kJ mol^{-1}.[19] Structures of these three compounds are given in Scheme 2. We have taken the same crystal structure of DNA and repeated the same procedure as followed for AODIQ (see Experimental section). The optimized docked conformations of these three compounds bound to DNA are presented in Figure 11. The figure reveals that all the three compounds bind to the minor groove of DNA at a very similar position to that of AODIQ (*cf.* Figure 10). The calculated docking energy for indoleamine, carbazole and pyrimido pyridoindole come out to be – 22.6 kJ mol^{-1}, – 26.3 kJ mol^{-1} and – 28.4 kJ mol^{-1} respectively. The estimated docking energy values of the compounds are in reasonable agreement with the value of the docking energy for AODIQ (– 30.5 kJ mol^{-1}). Thus, the comparative docking study suggests that AODIQ binds to the

ctDNA in the same binding mode and the similar binding site as the three known nervous system stimulants bind to the ctDNA and hence, projects AODIQ as a potential nervous system stimulant.

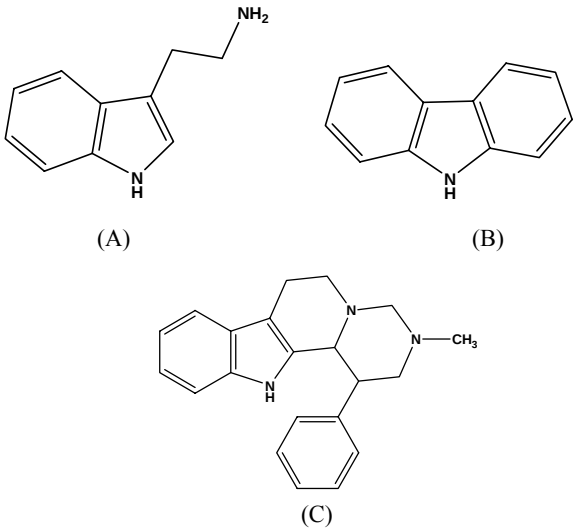

Scheme 2. Structures of indoleamine (A), carbazole (B) and pyrimido pyridoindole (C).

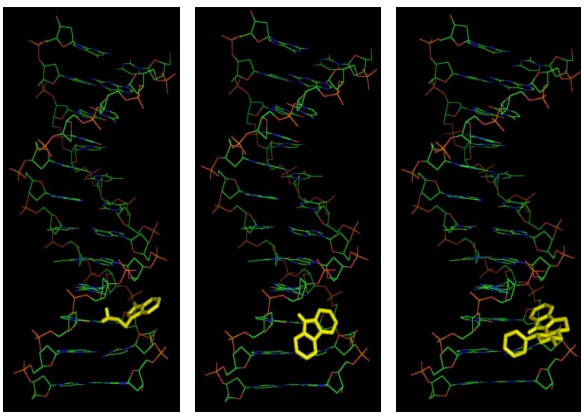

Figure 11. Optimized docked pose of indoleamine (A), carbazole (B) and pyrimido pyridoindole (C) bound to the minor groove of B-DNA.

Surfactant induced dissociation of the drug-DNA complex

The described sets of experiments together with the molecular docking simulation have convincingly established the mode of binding of the drug with the DNA. In this section, we have made an endeavor to investigate if surfactant can be employed to dissociate the drug from the drug-DNA complex for providing a new dimension to our objective of developing prospective strategies to get rid of drug induced adverse side effects, through the excretion of the drugs from the body.[27-30] The detergent-sequestration technique is capable of dissociating the drug-DNA complex by exploiting the detergent molecules (rather micelles) as the hydrophobic sink for the dissociated drug.[58-61] For the present purpose, we have opted for cationic surfactant cetyltrimethyl ammonium bromide (CTAB). The choice of the cationic surfactant over the anionic or non-ionic surfactants lies in the fact that the electrostatic attraction between the cationic surface charge of the surfactant and the negative phosphate backbone of DNA results in a closer approach between the two and hence, favors the interaction.[49] Although some groups have reported the interaction of CTAB on DNA to be non-destructive in nature so far as the secondary structure of DNA is concerned,[49,62] reports are there revealing that CTAB induces compaction in the DNA structure.[63,64] This is likely to favor the release of the drug from the DNA, specially when the former is bound through groove binding mode. Figure 12 depicts the changes in the emission profile of DNA-bound drug with the gradual addition of CTAB. With the increase in the CTAB concentration, the emission intensity of the DNA-bound AODIQ increases remarkably with a substantial hypsochromic shift of 24 nm (from 505 nm in 0.8 mM DNA to 481 nm in 1.05 mM CTAB). The fluorometric modifications of the drug (both the enhancement in the intensity and the blue shift of the emission maximum) with increasing concentration of the added CTAB are in well agreement with its behavior in pure CTAB micellar medium as reported earlier.[24] The agreement between the positions of the emission maximum of AODIQ in the present composite environment (DNA-bound AODIQ with added CTAB) and that in aqueous CTAB medium implies that after being released from the DNA, the drug molecules do not reside in the bulk aqueous phase, rather, they get entrapped into the micellar medium. Trapping of the drug in the CTAB micelle from the DNA environment is rationalized from a competitive binding of the probe, where the binding constant of the drug with CTAB micelle (4.4×10^5 M^{-1})[24] is two order of magnitude higher than that with ctDNA (1.2×10^3 M^{-1}, *vide infra*). The entrapment of the drug in the CTAB micellar environment is further established from the fluorescence anisotropy and time resolved fluorescence decay measurements.

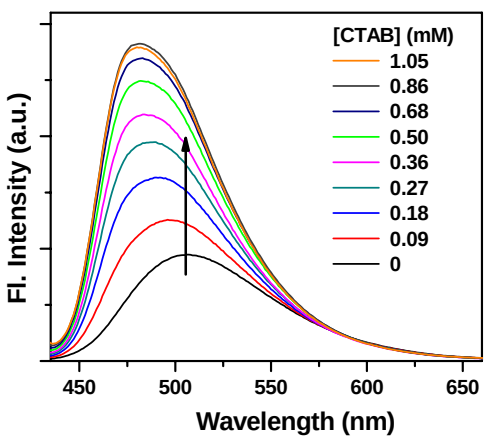

Figure 12. Emission spectra of DNA-bound AODIQ in presence of different concentrations of CTAB. The concentrations of the CTAB solutions are labeled in the legends. λ_{exc} = 420 nm, [DNA] = 0.8 mM.

As already discussed, steady state fluorescence anisotropy value provides information regarding the microenvironment imposed restriction on the rotational motion of a fluorophore, thereby indicating the location of the probe in a complex heterogeneous environment. The fluorescence anisotropy of the

drug in DNA environment decreases considerably from 0.21 to 0.16 upon addition of 1.05 mM CTAB. The anisotropy value of the DNA-bound drug in CTAB environment (0.16) agrees well with the value observed for AODIQ in aqueous CTAB medium (0.15).[24] The observation leads to the conclusion that after being released from the DNA, AODIQ gets entrapped into the CTAB micelle. The little higher value of anisotropy of DNA-bound AODIQ in CTAB medium (0.16) compared to that in the aqueous CTAB micellar phase (0.15) may be due to the increased bulk viscosity of the composite medium or due to the presence of both types of drug molecules (DNA-bound and micelle-entrapped) giving rise to an intermediate value of the fluorescence anisotropy.

To substantiate the dislodging of the drug from the DNA environment to the micelle, we have exploited the time resolved fluorescence study. Figure 13 depicts the decay profiles of the drug in different environments and the corresponding analyzed data are tabulated in Table 2. As already said, in aqueous buffer, the average lifetime of AODIQ is 0.93 ns. In 1 mM CTAB medium the decay is single exponential with a higher lifetime value of 1.58 ns, justifying the confinement of the probe within the micellar nanocavity. In DNA environment the drug shows biexponential decay with two different lifetime values ~ 0.9 ns and ~ 4 ns (*vide infra*). In the composite medium (DNA + CTAB), the drug exhibits a biexponential decay with two lifetime components 1.59 ns and 3.76 ns. The short lifetime component of the drug in the composite medium (1.59 ns) corresponds well to the value observed in aqueous CTAB medium (1.58 ns) and is assigned to the micelle-bound drug while the longer component is assigned to the DNA-bound drug. Thus, the above sets of experiments reveal that dissociation of the drug-DNA complex is possible by the addition of CTAB and the dissociated drug prefers to reside in the micellar environment.

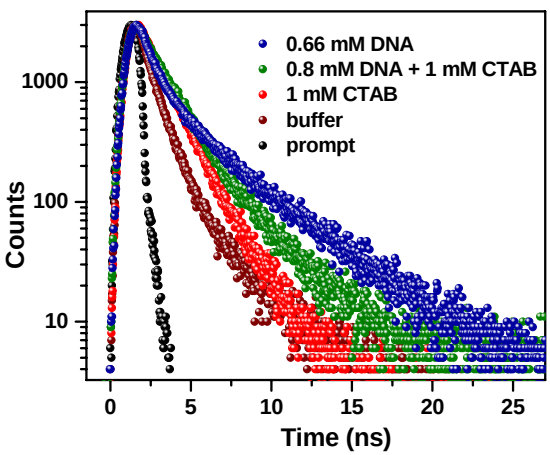

Figure 13. Time resolved fluorescence decay of AODIQ in different environments as mentioned in the legends monitoring at corresponding emission maxima. The sharp profile (black) on the left is the lamp profile. λ_{exc} = 370 nm.

Table 2. Time resolved fluorescence decay parameters of AODIQ in different environments

Medium	τ_1 (ns)	a_1	τ_2 (ns)	a_2	τ_{avg} (ns)	χ^2
buffer	0.84	0.95	2.59	0.05	0.93	1.05
1 mM CTAB	1.58	1.00			1.58	1.21
0.66 mM DNA	0.91	0.81	4.14	0.19	1.52	1.19
0.8 mM DNA + 1 mM CTAB	1.59	0.90	3.76	0.10	1.80	1.20

Conclusion

The present study articulates a spectroscopic exploration of the binding interaction of a β-carboline analogue, a potential nervous system stimulant, with calf-thymus DNA. The photophysical behavior of the drug molecule is significantly modified in the DNA environment compared to that of the aqueous buffer medium. The series of steady state and time resolved spectroscopic measurements together with the circular dichroism spectral study and DNA helix melting study unequivocally establish the mode of binding of the drug to be groove binding. This has also been corroborated from molecular docking simulation. CTAB induced sequestration of the DNA-bound drug presents a simple strategy to excrete the drug from the DNA environment. The present study is supposed to provide important insight in understanding the binding interaction of other imperative β-carboline drug molecules with DNA or similar biological targets through spectroscopic techniques.

Acknowledgements

Financial support from the C.S.I.R., Government of India, is gratefully acknowledged. P.K. and S.G. thank the Council of Scientific and Industrial Research and the University Grants Commission respectively for their research fellowships. We thank the reviewers for their constructive suggestions to improve the merit of the article.

Notes and references

[a] *Department of Chemistry, Jadavpur University, Kolkata - 700 032, India*
**Corresponding author: Fax: 91-33-2414 6584*
E-mail: nitin.chattopadhyay@yahoo.com (N. Chattopadhyay)
ghosh.saptarshi89@gmail.com (S. Ghosh)

1 S. E. Osborne and A. D. Ellington, *Chem. Rev.*, 1997, **97**, 349-370.
2 Y. Ma, G. Zhang and J. Pan, *J. Agric. Food Chem.*, 2012, **60**, 10867−10875.
3 Y. Fei, G. Lu and G. Fan, *Anal. Sci.*, 2009, **25**, 1333−1338.
4 X. L. Li, Y. J. Hu, H. Wang, B. Q. Yu and H. L. Yue, *Biomacromolecules*, 2012, **13**, 873−880.
5 L. Zhou, J. Yang, C. Estavillo, J. D. Stuart, J. B. Schenkman and J. F. Rusling, *J. Am. Chem. Soc.*, 2003, **125**, 1431−1436.
6 P. B. Dervan, *Biorg. Med. Chem.*, 2001, **9**, 2215-2235.
7 S. Das and G. S. Kumar, *J. Mol. Struct.*, 2008, **872**, 56−63.
8 I. Saha, M. Hossain and G. S. Kumar, *J. Phys. Chem. B*, 2010, **114**, 15278-15287.
9 D. Sahoo, P. Bhattacharya and S. Chakravorti, *J. Phys. Chem. B*, 2010, **114**, 2044−2050.
10 D. Bhowmik, M. Hossain, F. Buzzetti, R. D'Auria, P. Lombardi and G. S. Kumar, *J. Phys. Chem. B*, 2012, **116**, 2314−2324.

11 A. Ganguly, S. Ghosh and N. Guchhait, *Phys. Chem. Chem. Phys.*, 2015, **17**, 483-492.
12 E. Tuite and B. Nordén, *J. Am. Chem. Soc.*, 1994, **116**, 7548–7556.
13 R. Langer, *Science*, 2001, **293**, 58-59.
14 S. Stolc, *Life Sci*., 1999, **65**, 1943-1950.
15 A. Dias, A. P. Varela, M. G. Miguel, R. S. Becker, H. D. Burrows and A. L. Macanita, *J. Phys. Chem*., 1996, **100**, 17970-17977.
16 A. P. Varela, M. G. Miguel, A. L. Macanita, H. D. Burrows and R. S. Becker, *J. Phys. Chem*., 1995, **99**, 16093-16100.
17 A. Mallick, B. Haldar, S. Maiti, S. C. Bera and N. Chattopadhyay, *J. Phys. Chem. B*, 2005, **109**, 14675−14682.
18 N. Chattopadhyay, R. Dutta and M. Chowdhury, *J. Photochem. Photobiol. A*, 1989, **47**, 249-257.
19 F. A. Tanious, D. Ding, D. A. Patrick, R. R. Tidwell and W. D. Wilson, *Biochemistry*, 1997, **36**, 15315−15325.
20 V. Sniecks and R. H. F. Manske, *The Alkaloids*, R.H.F. Manske (Ed.), vol. 11, Academic Press, New York, 1968.
21 E. Schilitter and H. J. Bein, *Medicinal Chemistry*, E. Schilitter (Ed.), vol. 7, Academic Press, New York, 1967.
22 A. Mallick, S. Maiti, B. Haldar, P. Purkayastha and N. Chattopadhyay, *Chem. Phys. Lett.*, 2003, **371**, 688-693.
23 A. Mallick, B. Haldar and N. Chattopadhyay, *J. Phys. Chem. B*, 2005, **109**, 14683−14690.
24 A. Mallick, B. Haldar, S. Maiti and N. Chattopadhyay *J. Colloid Interface Sci.*, 2004, **278**, 215-223.
25 P. Das, A. Chakrabarty, B. Haldar, A. Mallick and N. Chattopadhyay, *J. Phys. Chem. B*, 2007, **111**, 7401−7408.
26 P. Das, D. Sarkar and N. Chattopadhyay, *Chem. Phys. Lipids*, 2008, **154**, 38-45.
27 D. Sarkar, D. Bose, A. Mahata, D. Ghosh and N. Chattopadhyay, *J. Phys. Chem. B*, 2010, **114**, 2261-2269.
28 B. Jana, S. Ghosh and N. Chattopadhyay, *J. Photochem. Photobiol. B: Biol.*, 2013, **126**, 1-10.
29 S. Ghosh, S. Chattoraj and N. Chattopadhyay, *Analyst*, 2014, **139**, 5664-5668.
30 P. Kundu, S. Ghosh, B. Jana, and N. Chattopadhyay, *Spectrochim. Acta, Part A*, 2015, **142**, 15-24.
31 V. S. Giri, B. C. Maiti and S. C. Pakrashi, *Heterocycles*, 1984, **22**, 233-236.
32 B. Jana, S. Senapati, D. Ghosh, D. Bose and N. Chattopadhyay, *J. Phys. Chem. B*, 2012, **116**, 639−645.
33 J. R. Lakowicz, *Principles of Fluorescence Spectroscopy*, 3rd Edn., Springer, New York, 2006.
34 H. R. Drew, R. M. Wing, T. Takano, C. Broka, S. Tanaka, K. Itakura and R. E. Dickerson, *Proc. Natl. Acad. Sci. U.S.A.*, 1981, **78**, 2179−2183.
35 O. Trott and A. J.Olson, *J. Comput. Chem.*, 2010, **31**, 455-461.
36 D. Seeliger and B. L. de Groot, *J. Comput. Aided Mol. Des.*, 2010, **24**, 417- 422.
37 M. W. Chang, C. Ayeni, S. Breuer and B. E. Torbett, *PLoS One*, 2010, **5:e11955**, 1-9.
38 M. J. Frisch, G. W. Trucks, H. B. Schlegel, G. E. Scuseria, M. A . Robb, R. J. Cheeseman, J. A. Jr. Montgomery, T. Vreven, K. N. Kudin, J. C. Burant et al. *Gaussian 03*, revision E.01; Gaussian, Inc.: Wallingford, CT, 2004.
39 W. L. De Lano, *The PyMOL Molecular Graphics System,* De Lano Scientific: San Carlos, CA, 2004.
40 S. S. Mati, S. S. Roy, S. Chall, S. Bhattacharya and S. C. Bhattacharya, *J. Phys. Chem. B*, 2013, **117**, 14655−14665.
41 S. Bhattacharya, G. Mandal and T.Ganguly, *J. Photochem. Photobiol. B: Biol.*, 2010, **101**, 89−96.
42 D. Sarkar, P. Das, S. Basak and N. Chattopadhyay, *J. Phys. Chem. B*, 2008, **112**, 9243−9249.
43 A. Mallick, S. C. Bera, S. Maiti and N. Chattopadhyay, *Biophys. Chem*., 2004, **112**, 9-14.
44 E. M. Kosower, H. Dodiuk, K. Tanizawa, M. Ottolenghi and N. Orbach, *J. Am. Chem. Soc.*, 1975, **97**, 2167-2178.
45 C. Reichardt, *Molecular Interactions*; H. Ratajazak, Orville Thomas, W. J. Eds. Wiley: New York, 1982, **3**.
46 H. A. Benesi and J. H. Hildebrand, *J. Am. Chem. Soc.*, 1949, **71**, 2703−2707.
47 S. Das and G. S. Kumar, *J. Mol. Struct.*, 2008, **872**, 56−63.
48 I. Saha, M. Hossain and G. S. Kumar, *J. Phys. Chem. B*, 2010, **114**, 15278-15287.
49 B. K. Paul and N. Guchhait *J. Phys. Chem. B*, 2011, **115**, 11938−11949.
50 A. Mahata, D. Sarkar, D. Bose, D. Ghosh, A. Girigoswami, P. Das and N. Chattopadhyay, *J. Phys. Chem. B,* 2009, **113**, 7517-7526.
51 D. Sarkar, A. Mahata, P. Das, A. Girigoswami, D. Ghosh and N. Chattopadhyay, *J. Photochem. Photobiol. B: Biol.*, 2009, **96**, 136−143.
52 S. Ghosh, P. Kundu, B. K. Paul and N. Chattopadhyay, *RSC Adv.*, 2014, **4**, 63549-63558.
53 K. van Holde, W. C. Johnson and P. S. Ho, *Principles of Physical Biochemistry*; Prentice Hall: New York, 1998.
54 S. S. Wijeratne, J. M. Patel and C. H. Kiang, *Rev. Plasmonics*, 2012, **2010**, 269−282.
55 S. J. Campbell, N. D. Gold, R. M. Jackson and D. R. Westhead, *Curr. Opin. Struct. Biol.*, 2003, **13**, 389–395.
56 C. G. Ricci and P. A. Netz, *J. Chem. Inf. Model.*, 2009, **49**, 1925-1935.
57 J. Reedijk, *Proc. Natl. Acad. Sci. USA*, 2003, **100**, 3611-3616.
58 W. Muller and D. M. Crothers, *J. Mol. Biol.*, 1968, **35**, 251–290.
59 F. Westerlund, L. M. Wilhelmsson, B. Nordén and P. Lincoln, *J. Am. Chem. Soc*., 2003, **125**, 3773–3779.
60 E. J. Gabbay, D. Grier, R. E. Fingerle, R. Reimer, R. Levy, S. W. Pearce and W. D. Wilson, *Biochemistry*, 1976, **15**, 2062–2070.
61 D. W. Wilson, D. Grier, R. Reimer, J. D. Bauman, J. F. Preston and E. J. Gabbay, *J. Med. Chem.*, 1976, **19**, 381–384.
62 S. Ghosh, D. Banik, A. Roy, N. Kundu, J. Kuchlyan and N. Sarkar, *Phys. Chem. Chem. Phys.*, 2014, **16**, 25024-25038.
63 R. S. Dias, L. M. Magno, A. J. M. Valente, D. Das, P. K. Das, S. Maiti, M. G. Miguel and B. Lindman, *J. Phys. Chem. B*, 2008, **112**, 14446−14452.
64 S. Husale, W. Grange, M. Karle, S. Bürgi and M. Hegner, *Nucleic Acids Res*. 2008, **36**, 1443-1449.

TABLE OF CONTENTS

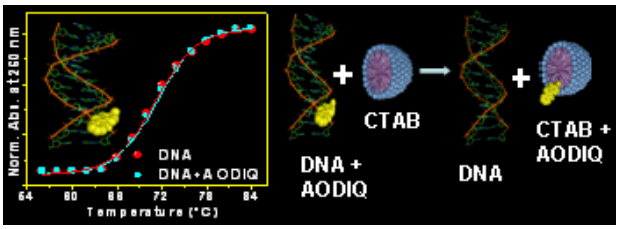

Binding interaction of a potential nervous system stimulant with calf-thymus DNA has been divulged exploiting various spectroscopic techniques as well as molecular docking simulation. Further, dissociation of the drug from the drug-DNA complex has been achieved by the detergent sequestration method.